QUANTIFYING FORCE ON THE BODY WHILE HEAD-LOADING

Natalie Dean
Massachusetts Institute of Technology
Cambridge, MA, US

ABSTRACT

Roughly 17 million women and children in Sub-Saharan Africa are responsible for traveling over 30 minutes to collect clean drinking water for them and their families, making understanding the biomechanics and potential health impacts of head-loading vital [2]. Forces on the foot and head while head-loading a 20 liter jerry can filled with water at speed and incline conditions of 2.4 to 3.9 km/h and 0 to 10 degrees were measured utilizing force pads attached to the heel of the foot, ball of the foot, and underside of the jerry can. An increase in speed also increased loading on the heel of the foot. A net increase in loading on the ball of the foot was observed with an increase in incline from 0 to 10 degrees, but a net decrease in loading on the heel of the foot. A shift in primary loading from the heel to the ball of the foot was determined to occur around the 8.5 degree mark resulting from either experimental setup error or posture shift.
Keywords: gait cycle, head-loading, biomechanics, water hauling

INTRODUCTION

Across Sub-Saharan Africa (SSA), roughly 17 million women and children are responsible for collecting and transporting water for more than 30 minutes to provide access to clean water for them and their families [1]. The act of water hauling is both inherently gendered and dangerous, upheld by gender norms and resulting in frequent injury. With regards to the gendered division of labor, it is often a source of pride among men to not have to collect water, as it implies a large family and good work ethic [2]. Furthermore, when men do participate in water collection activities, it is usually under the circumstances of assisting his wife, rather than an ordinary activity [2]. Additionally, there is a gendered component in the form of water transportation. While men are permitted to utilize bikes as a form of intermediate water hauling technology, it is culturally inappropriate for women to do the same and they resort to head-loading (used here to describe walking with a mass of water in a container carried on the top of the head) [2]. Long term head-loading during water collection can lead to chronic and serious physical health conditions [3]. Given the high number of women and children responsible for water collection (particularly those that utilize head-loading as a method of transportation) and its associated high rates of injury, understanding the biomechanics of head-loading water could be vital information in the prevention or treatment of these health conditions.

To determine the relationship between applied load and the load experienced by various parts of the body, force pads will be placed underneath the chosen water receptacle (in this case a standard 20 liter jerry can) and attached to the underside of the feet of the carrier. The load will remain constant with the jerry can being completely filled with water and held on top of the head. Using a treadmill, incline and speed will be varied from 0 to 10 degrees and 2.4 to 3.9 km/h respectively. The force sensor data will be mapped to positions in the gait cycle using force calculations to provide verification (ex: if force on the left foot is high, force on the right foot is zero, and force on the head is constant, it can be inferred that the carrier is in the toe-off or midstance phase of the gait cycle wherein only one foot is in contact with the ground). Using this mapped data and kinematic relationships across all the trials at varied inclines and speeds, a mathematical relationship between gait cycle, incline, speed, applied load, and experienced load (on each of the feet and the head) can be extrapolated.

BACKGROUND

THE NECESSITY OF WATER HAULING AND ITS IMPACTS ON THE BODY

Water scarcity is defined as the condition of inadequate supply of water compared to its demand and can be broken up into two primary categories, physical and economic scarcity [7]. In SSA, the prevalence of water scarcity is due mostly to economic constraint, although climate change, population growth, environmental overexploitation is increasing the rate of physical scarcity [7], which has led to an estimated two-thirds of the population leaving their homes to collect water [8]. Despite so many people (predominantly women and children) having water collection as an everyday part of life SSA, in-depth analyses into the energy expenditure and biomechanics of gendered domestic tasks are limited and difficult [9]. Although head-loading allows for increased balance over uneven terrain, the prevalence of serious health conditions increases, including arthritis (notably osteoarthritis), tumoral calcinosis (calcification of soft tissue around the joints), degenerative disc disease (degradation of the cartilage in the vertebrae), spondylolisthesis (misalignment of the vertebrae), neurological deficits, numbness and loss of feeling in the arms, flattening of the lordotic (spinal) curve, neck stiffness and pain, metatarsal stress fractures, miscarriages, premature births and low birth weight, reproductive organ prolapses, and reduced fertility [3-6, 10]. Given the necessity of head-loading for so many people (with no end in the foreseeable future), it is critical to understand how force from head-loading may be distributed onto or absorbed by various parts of the body, especially the head and feet.

THE BIOMECHANICS OF WALKING (AN EXPLANATION OF THE GAIT CYCLE)

Figure 1 depicts the gait cycle (a person's walking pattern) which can be broken up into two main parts, the stance phase (some or all of the foot is in contact with the ground and weight is supported) and the swing phase (none of the foot is in contact with the ground and body weight is on the ground contacting foot) [11].

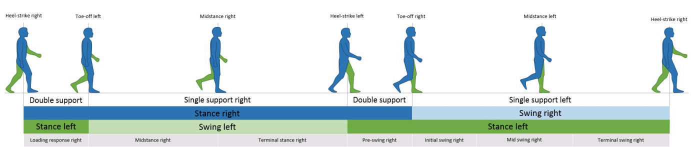

Figure 1: A breakdown of the human gait cycle into the stance/swing phases and single/double support phases. Physiopedia.

Within the stance phase are the heel strike (heel contacts ground), loading response (ball of foot contacts ground), midstance (body weight transfer), terminal stance (heel off of ground), and pre-swing (heel off the ground) phases [11]. During the stance phase, load on the foot shifts from the heel to the toe as shown in Figure 2.

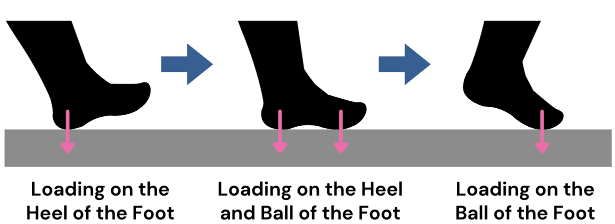

Figure 2: Loading changes on the foot between the heel strike and toe-off.

After preparing to leave the ground and transferring load, the foot enters the swing phase which is divided into three parts: initial swing, mid-swing, late swing [11]. Another way to describe the actions of the feet during the gait cycle is through double and single support periods. Single support periods encompass a majority of a person's walking time where only one foot is in contact with the ground and supports all of the applied load. In double support periods, both feet are in contact with the ground, however most of the time during double support periods the load will not be evenly distributed as weight shifts with the swinging motion of the legs. Similarly, when a foot is in contact within the ground, loading over a single foot will vary with position in the gait cycle. While in the toe-off portion of the gait cycle, loading is concentrated on the ball of the foot and toes versus the heel-strike phase in which loading is concentrated on the heel of the foot.

It is important to note that gait cycle patterns differ greatly by age, sex, and individual physical characteristics. In general, females have greater loading on the lateral column of the foot (the side of the foot closest to the fifth or pinky toe) when compared to males. However, males have a greater force-time integral (impulse) over the entire foot [12]. It is also important to note that changes in head position or loading may occur during the gait cycle due to an individual's stance or disability [12].

THE MECHANICS OF INCLINES AND LOADS

The use of classical mechanics knowledge allows for the creation of a rough model displaying the relationship between incline and force on the feet while walking, as shown in Figure 3. For this rough estimation, at a single moment in time, a person head-loading an object of constant mass can be modeled as two discrete uniformly dense objects at rest on an incline where one object is centered on the top of the other. Equations 1 through 7 display the mathematical calculations to determine: (1) the weight of the head-loaded object, (2) the normal force of the head-loaded object, (3) the weight of the head-loading person, (4) the total applied force, (5) the normal force produced by the total applied force, (6) the static friction force between the ground and head-loader's foot, and (7) the downhill force of the mass-person system. The applied force (the force enacted on the ground by the foot) can thus be derived from the weight of the person, the weight of the object being head-loaded, and the angle of incline. Opposing the applied force, is the force exerted by the ground on the foot is known as the applied normal force which is exactly equal to (but opposite of) the applied force. This normal force can then be used to determine the static friction force (which is opposed by the downhill force) by factoring in the coefficient of friction between the ground and bottom of the foot. While the downhill and friction force are not directly relevant for the scope of this study, they provide a more complete view of the biomechanics of head-loading and may be relevant for future work.

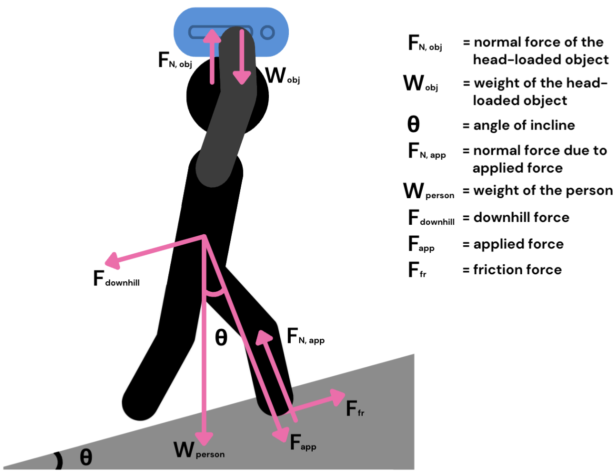

Figure 3: A simplified model of the forces acting in the body-incline-mass system while a walking person head-loads a mass and one foot is in contact with the ground.

$$W_{obj} = -m_{obj}g \quad (1)$$

$$F_{N,obj} = -W_{obj} \quad (2)$$

$$W_{person} = -m_{person}g \quad (3)$$

$$F_{app} = (W_{person} + W_{obj})cos\theta \quad (4)$$

$$F_{N,app} = -F_{app} \quad (5)$$

$$F_{fr} = \mu F_{N,app} \quad (6)$$

$$F_{downhill} = (W_{person} + W_{obj})sin\theta \quad (7)$$

Using the model as the basis for understanding work (as defined by Equation 8), it can be more easily understood why it feels physically harder to walk up an incline than across a horizontal plane. Work, understood in this case as the amount of energy necessary to move both the person and head-loaded object, is proportional to the normal force of the applied force and the distance traveled. As the angle of incline increases, the amount of force applied perpendicular to the walking surface decreases, creating a "disparity" between the energy available and the energy necessary to move [13]. Based on the simplified model and knowing that the person-object system is at equilibrium where no net change in horizontal position occurs, an additional source of work must exist to "balance" this disparity. This source of energy must thus be derived from the dynamic part of the system, the head-loading person. Equations 9 and 10 display the relationship between angle of incline, vertical position change, extra force needed from the body, and work done by the body while head-loading up a slope. As the angle of incline increases, a higher amount of energy must be supplied by the person's muscles to resist the Earth's gravitational force, so walking will feel more physically taxing. While work done by the body was not measured during this experiment, Equation 10 lends itself to a more complete understanding of the body's activities while head-loading.

$$W = \int_{y=a}^{y=b} F dy \quad (8)$$

$$F_{body,extra} = (W_{person} + W_{obj})(1 - cos\theta) \quad (9)$$

$$W_{body,extra} = \int_{y=a}^{y=b} (W_{person} + W_{obj})(1 - cos\theta)dy \quad (10)$$

Figure 4 focuses solely on the interactions between the bucket and the top of the head and details how the load applied to the head changes in a repeatable pattern following the up and down movements associated with walking. During the swing phase of the gait cycle when a foot swings forward to contact the ground, there is a slight parabolic motion of the head that follows the path of the foot. As the foot swings from the back position to the front of the body (upswing), the head moves up. When the foot is in the front position and drops to contact the ground (downswing), the head dips back downwards. In the upswing portion of the gait cycle, the weight of the object opposes the direction of acceleration and motion, thereby increasing force on the head (calculated by Equation 11). In the downswing portion of the gait cycle, the weight of the object aligns with the direction of acceleration and motion, thus decreasing the force on the head (calculated by Equation 12). While likely insignificant at small masses and head position changes, a heavy enough head-loaded mass or large change in head position could cause measurable force fluctuations during upswing and downswing.

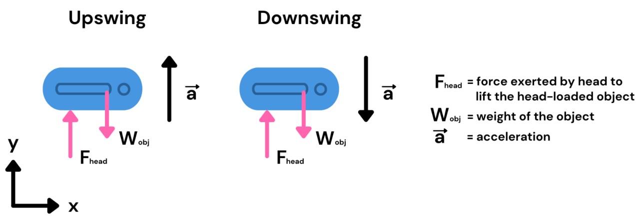

Figure 4: A simplified free body diagram of a head-loaded object during the upswing and downswing phases of the gait cycle.

$$F_{head} = m_{obj}\vec{g} + m_{obj}\vec{a} \quad (11)$$
$$F_{head} = m_{obj}\vec{g} - m_{obj}\vec{a} \quad (12)$$

EXPERIMENTAL DESIGN

SET UP

Figure 5 details the placement of force pads along the foot, jerry can, and general testing set up. A standard 20 liter high-density polyethylene jerry can filled with water weighing approximately 20 kilograms was selected as the head-loaded object to simulate a realistic the conditions carried by people responsible for water collection. Similar style jerry cans are common water carrying vessels in water scarce regions where water hauling is necessary because of their high availability, low price, pour spouts, handles, and durability. An Interlink FSR 406 force sensing resistor pad was attached to the side of the jerry can instead of the bottom due to the curvature of the bottom which could have skewed results or broken the sensor. During testing, the jerry can was turned 90 degrees so that the force pad sat between the top of the head and the side of the jerry can (held in place using the bottom and handle) to measure the impact of incline and speed on average maximum force on the top of the head. In addition, Interlink FSR 406 force sensing resistor pads were attached to the ball and heel of the left foot over the sock using athletic tape before being placed inside of an athletic shoe. Due to the fragility of the force pads, placement inside the shoe was necessary to eliminate harm that repeat contact with the rough walking surface of the treadmill could cause. The force pads on the ball and heel of the foot were used to measure how force over different regions of the foot experience loading and the impact of incline and speed on this loading. The wires of the force pads on the foot were secured to the leg to provide strain relief using athletic tape. All three force pads were then connected to a Vernier LabQuest Mini (which was secured at the chest region) leading to a computer collecting force data via Logger Pro.

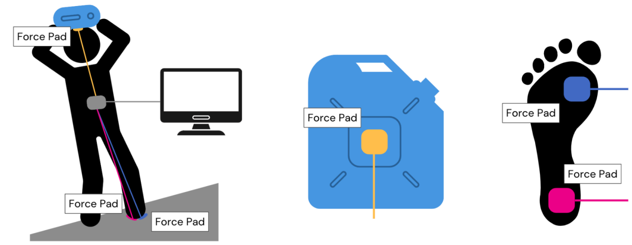

Figure 5: Force pad placement and electronics connections.

DATA COLLECTION

Data was recorded for 45 seconds at speeds of 2.4 to 3.9 km/h and at inclines of 0, 4, and 10 degrees from the horizontal. Test speeds were chosen based on the halved average walking speed for women in the 20-29 year old age range and then increased in 0.5 km/h increments until it became difficult to keep up with the speed of the treadmill while head-loading the filled jerry can [14]. The angles of incline were chosen based on general hiking standards to mimic totally flat, easy, and moderate trails [15]. The 10 degree incline was also chosen, in part, because an angle becomes significant in trigonometric calculations at about 10 degrees while still being attainable on a commercially available treadmill.

To collect data, the treadmill speed and incline were set, Logger Pro was set to collect for 45 seconds, and the jerry can was lifted onto the head with the force pad centered on the top of the head. To account for any initial gait inconsistencies and brief adjustment periods when starting on the treadmill, only data after the 15 second mark was utilized. The collection software automatically ceased after 45 seconds and, only after collection had ended, would the treadmill be turned off and the head-loaded jerry can removed.

Before each collection event, the force sensors were calibrated using a Vernier Force Plate. In this calibration procedure, a force pad would be pressed on using constant pressure from the hand or foot in short intervals against the force plate. The force pad outputs were then plotted against the force plate's readings to obtain the exponential relationship between recorded voltage and experienced force. Because data collection took place in two discrete events in which all of the 0 and 4 degree incline tests were completed and then the 10 degree incline tests, two sets of calibration data were produced and utilized to convert their respective voltage outputs to force.

Figure 6 displays the data points, fitted curves, and mathematical formulas to convert from voltage to force for the force pads on the top of the head, heel of the foot, and ball of the foot for the 0 and 4 degree incline tests. Figure 7 displays the data points, fitted curves, and mathematical formulas to convert from voltage to force for the force pads on the top of the head, heel of the foot, and ball of the foot for the 10 degree incline tests.

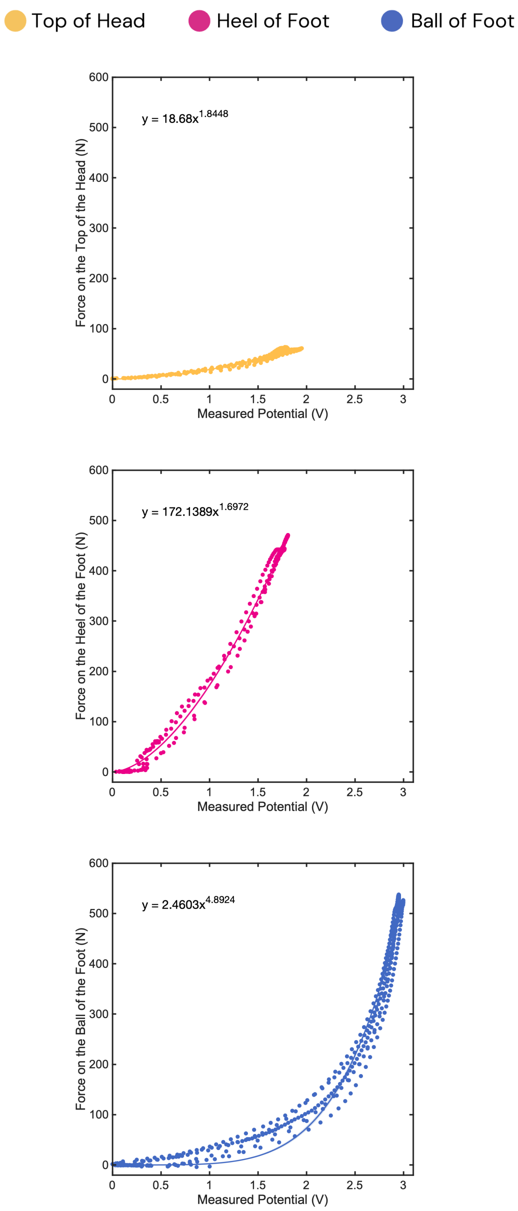

Figure 6: Top of the head, heel of the foot, and ball of the foot force pad calibration curves for the 0 and 4 degree incline tests.

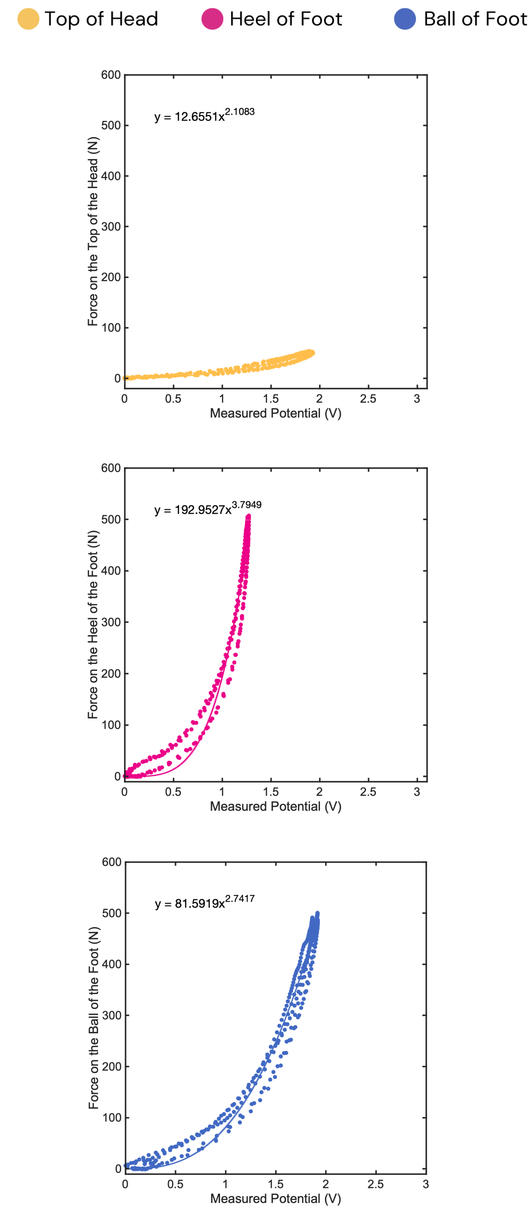

Figure 7: Top of the head, heel of the foot, and ball of the foot force pad calibration curves for the 10 degree incline tests.

RESULTS AND DISCUSSION

PREDICTED RESULTS

Equation 13 displays the correlation between vertical head acceleration, displacement, and movement frequency. Operating under the assumption that incline does not alter vertical head displacement or frequency and approximations of these values from the findings of a prior study (16), it can be determined that at all test conditions, the idealized maximum vertical head acceleration was 0.80 m/s^2.

$$\vec{a} = 4\pi^2 d f^2 \quad (11)$$

Vertical Head Movement Frequency: 2.0Hz
Vertical Head Displacement (Zero to Peak): 0.0050m
Measured Force of Person: 563.0N
Measured Force of Filled Jerry Can: 218.4N

While operating under the assumptions of the simplified model depicted in Figures 3 and 4, a set of predicted results can be calculated from Equation 13, the measured force of the head-loading person, the measured force of the head-loaded jerry can, and the angle of incline.

Table 1: Expected maximum force on the top of the head, minimum force on the top of the head, and maximum force on the foot per the simplified model by angle of incline.

Force	Equation	Expected Result (0 deg Incline)	Expected Result (4 deg Incline)	Expected Result (10 deg Incline)
Maximum Applied Force on the Foot	$F_{app} = (W_{person} + W_{obj})cos\theta$	781.4 N	779.5 N	769.5 N
Maximum Force on Head	$F_{head} = m_{obj}\vec{g} + m_{obj}\vec{a}$	236.0 N		
Minimum Force on Head	$F_{head} = m_{obj}\vec{g} - m_{obj}\vec{a}$	200.8 N		

TRIAL-LEVEL FORCE DATA TRENDS AND INITIAL ANALYSIS

Preliminary force pad analysis confirmed prior research knowledge that loading on the ball of the foot, heel of the foot, and top of the head create waveforms that correspond to the motions of the body during the gait cycle. Figure 8 displays sample force pad data from one trial of a 0 degree incline, moderate speed test, showing definitive maximum force values that correlate to the heel-strike (pink) and toe-off (blue) phases. Interestingly, smaller peaks were visible between the ball and heel of the foot peaks, indicating routine load transfer or posture shift during normal gait cycle movements.

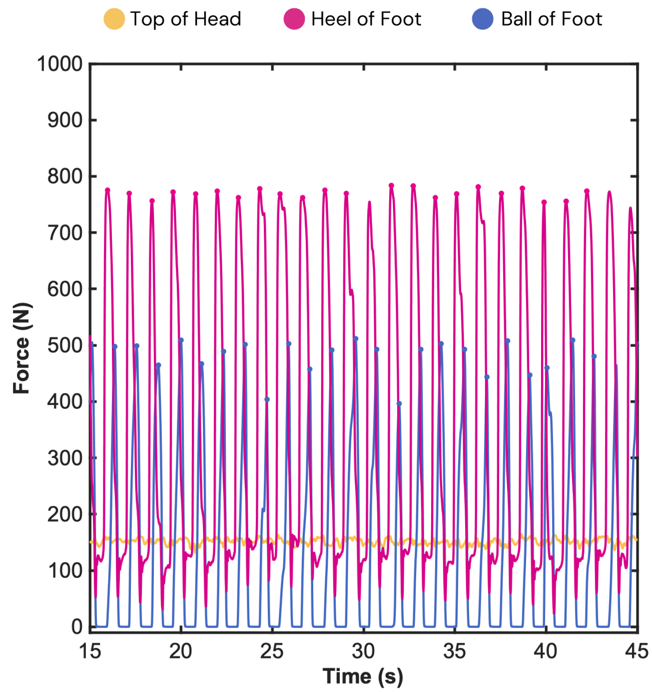

Figure 8: Top of the head, heel of the foot, and ball of the foot force pad data from trial 1 of the 0 degree incline, 3.4 km/h test.

Figure 9 displays data for the three force pads over several cycles of the gait cycle, highlighting regions to show in greater detail when a certain part of the foot is in contact with the floor as well as local maximums. Upon inspection, only very small fluctuations in force on the top of the head were found. Because of this, the maximums were not used when computing speed and incline trends like the heel and ball of the foot data were. Instead, the entire data set was averaged to receive a more accurate representation of the force exerted on the top of the head while head-loading. This trend of near zero force change while walking with respect to time was constant across all conditions tested. From this, it can be concluded that for uniformly dense head-loaded objects up to approximately 25 kilograms at 2.4 to 3.9 km/h and inclines ranging from 0 to 10 degrees, fluctuations in force on the head due to gait cycle mechanics are insignificant.

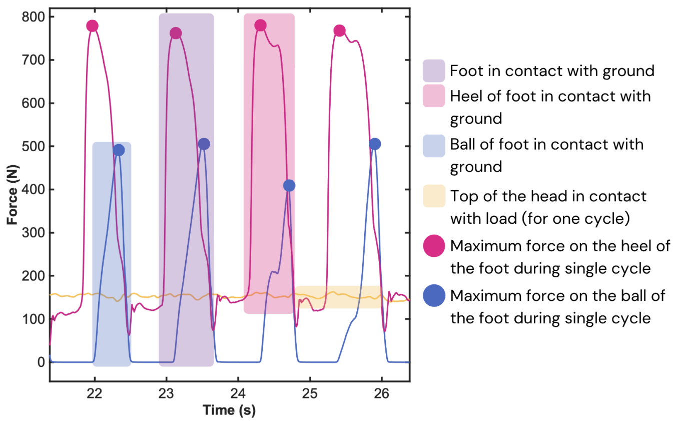

Figure 9: Five and a half second interval of force pad data from trial 1 of the 0 incline, 3.4 km/h test detailing portions of the gait cycle.

Figure 10 displays an example of an interesting phenomenon that occurred among all of the 0 and 4 degree incline tests in which the heel of the foot spends very little time at zero force like the ball of the foot does. This was an unexpected result as the force vs time waveform for the heel of the foot should have more closely modeled that of the ball of the foot, likely resulting from differences in calibration or experimental setup. This hypothesis is supported by the fact that the force minimum differences end at the beginning of the 10 degree incline tests which were conducted on a different day and thus utilized different calibration metrics and could have had slight differences in experimental set up.

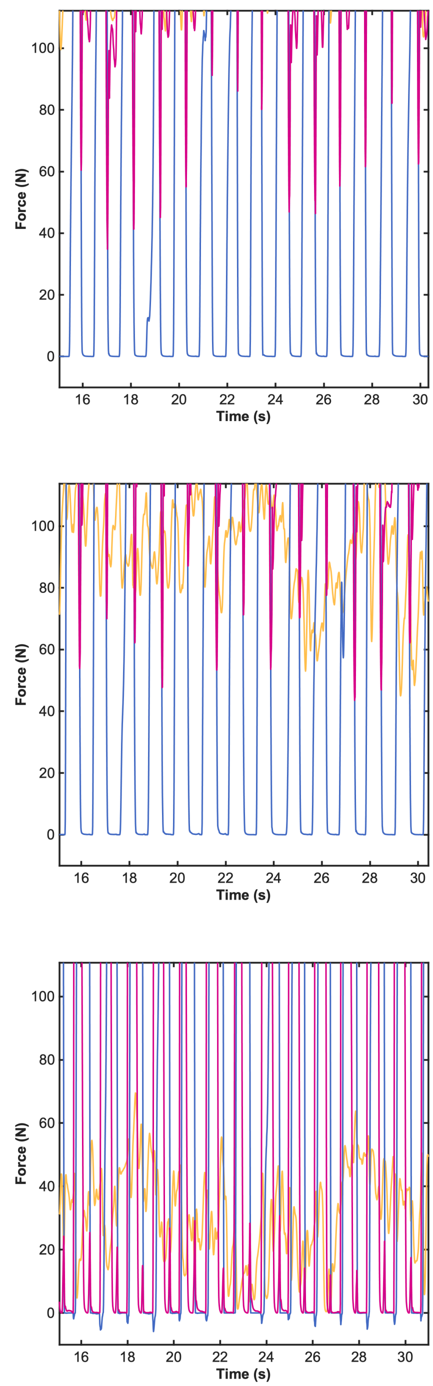

Figure 10: A comparison of the time spent at zero force on the heel of the foot for the first trial of the 0, 4, and 10 degree incline, 3.9 km/h tests.

EXPERIMENTAL RESULTS

To analyze broader biomechanical trends, the maximum force value for each occurrence of the gait cycle for each sensor over the 30 second trial interval was found and then averaged. Because of the low variance in force on the top of the head, the entire data set was averaged for this sensor. This averaging process was repeated for the three trials for each test. Using this method, 12 unique datasets were created, one for each speed-angle condition tested. Each data set included the average and its uncertainty for each sensor (top of the head, heel of the foot, and ball of the foot) at the specified speed and incline. This data was then plotted and fitted with either a linear or piecewise model. Figure 11 shows three graphs plotting the maximum force values for each of the three sensors at constant incline over varying speeds. Analyzing these graphs shows that no statistical difference in force on the head occurs as a result of incline or speed. Despite the average experimental value for force on the top of the head being significantly lower than the simplified model's expected value (measured at 113.09 ± 67 Newtons), measured maximum loading on the foot was consistent with the expected values for all slopes tested, validating the created model. Interestingly, while loading on the heel of the foot increases with speed at constant incline, loading on the ball of the foot does not. A possible explanation for this is that as speed increases, loading over the entire foot does increase, but a bulk of the force is absorbed by the first point of contact. This would explain, then, the upwards trend in loading on the heel even after the switch of primary loading from the heel to the ball of the foot seen in the 10 degree incline graph.

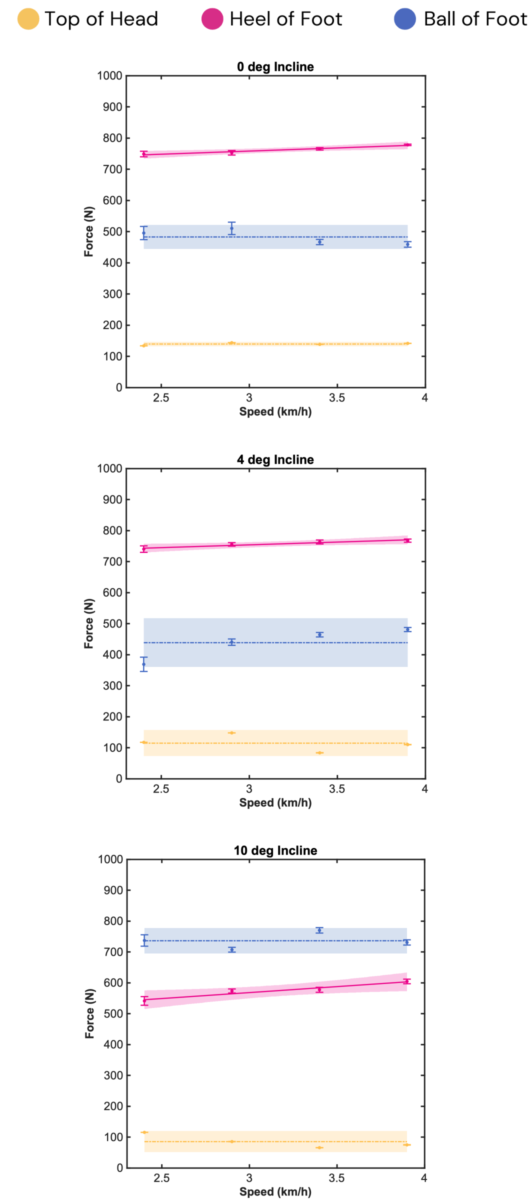

Figure 11: A comparison of average maximum force on the top of the head, heel of the foot, and ball of the foot by incline while head-loading at varying walking speeds.

Figure 12 shows the averaged data at constant speed over varying inclines. By reformatting the data and fitting a piecewise model to the points, a relationship between angle and loading over the foot can be constructed. Around the 8.5 degree incline mark, primary loading on the foot switches from the heel to the ball of the foot, represented by the intersection of the two functions. There are several possibilities for how such a radical shift in loading occurred with the first explanation being similar to that of the minimum loading of the heel during the 0 and 4 degree tests. Calibration or placement on the foot of the force pads before the 10 degree incline test could have been different enough to skew the results and cause this perceived shift in loading. It is known from prior experience that crossing of the force pad wires or improper contact between the foot and inside of the shoe can dramatically alter results. A non-erroneous explanation, however, includes a change in posture that occurs between 4 and 10 degrees that is the body's way of adjusting to the incline. Background research indicates that to walk up an incline, a person often shifts their center of gravity forwards to resist the downhill force and avoid falling backwards. When head-loading, it is not uncommon for long term exposure to result in flattening of the lordotic curve, a change in spinal anatomy that protrudes the stomach outward. This anatomical change pushes the center of mass more forward and (in theory) makes it easier to climb uphill without leaning forward as much, further supporting the posture change theory.

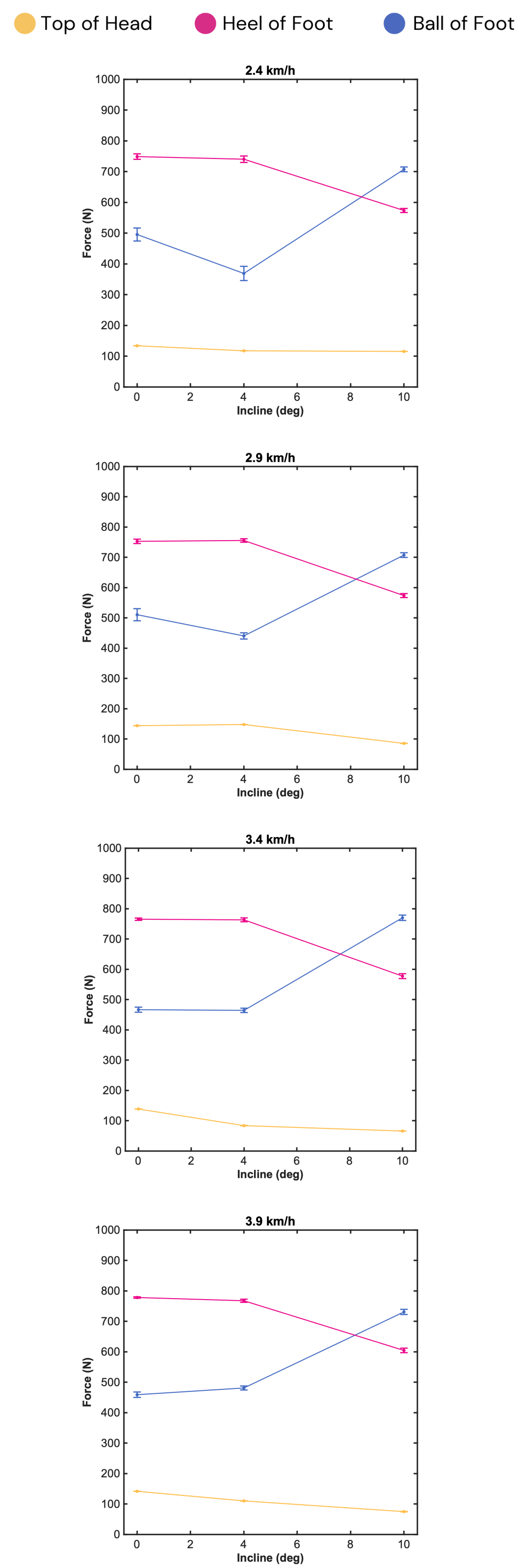

Figure 12: A comparison of the average maximum forces on the top of the head,

heel of the foot, and ball of the foot at constant speed and varying incline.

FUTURE STEPS AND REVISIONS

Should the experiment be repeated, the range of inclines should be expanded and more evenly spread out. Ideally, the angles 0, 4, 8, and 12 degrees from the horizontal would be tested to determine if the primary loading switch observed at about 8.5 degrees is realistic. While the range of speeds seems sufficient to mimic the walking conditions capable of the average human head-loading a 20 liter jerry can of water, more test subjects of diverse identities (including age and gender) should be tested. Given the differences in loading on the foot by sex as well as the gendered divide in water-hauling via head-loading, comparing results between male and female test groups could provide valuable insights. In addition, it is recommended that all testing either occurs with the same experimental set up or that a more sophisticated method of placing force pads is devised to reduce potential sources of error. It should be noted that this experiment was extremely limited in terms of the number of test subjects, friction force, and variability in the mass of the object head-loaded. Only one subject was observed, so data could have been skewed by individual anatomy or disability. The coefficient of friction between shoes and treadmill fabric is extremely high and, with higher friction, a person spends less energy fighting the downhill force produced by the slope which may have impacted loading over the foot. Different terrains could provide interesting metrics on the bodily response of an individual while head-loading. Only one object with a mass of approximately 20 kilograms was tested to limit the number of variables, but it is possible that posture and loading on the body can be manipulated through a combination of speed, incline, and object mass. To further back up findings, spinal compression and posture could provide insight into determining if there is a generalized set of "safe" conditions to travel at while head-loading to minimize damage to the body.

CONCLUSION

Results indicate a slight but significant dependance of loading on the heel of the foot on speed for low angles (0, 4, and 10 degrees) at moderate walking pace (2.4 to 3.9 km/h) during head-loading of a roughly 20 kilogram object. Force changes at these conditions on the top of the head are negligible with respect to both incline and speed. Similarly, loading on the ball of the foot appears to be independent of speed and become the primary source of loading on the foot around the 8.5 degree mark, but further testing is needed to confirm if this is due to error or biomechanical changes. Posture, anatomy, sex, and disability may impact results of loading on the foot should be considered when devising a model to calculate the biomechanics of head-loading on the body, but treatment of the body-object-slope system as a static model for an instantaneous moment in time seems to generally hold up under empirical testing.

ACKNOWLEDGMENTS

The author would like to thank the following groups and individuals for their contributions to the inspiration, development, and/or execution of this experiment and presentation: the 2.671 instruction team (in particular Dr. Barbara Hughey, Professor Thomas Peacock, Sarah Bates, and Claire Berman), Erik Kondo, Eric Noriega, and Danielle Bergstrom.

REFERENCES

[1] George Washington University Milken Institute School of Public Health, "17 Million Women/Children Tasked with Household Water Collection in 24 African Countries." [Online]. Available: https://www.sciencedaily.com/releases/2016/06/160601151920.htm. [Accessed: 24-Sep-2024].
[2] Van Houweling, E., ""A Good Wife Brings Her Husband Bath Water": Gender Roles and Water Practices in Nampula, Mozambique." [Online]. Available: https://www.tandfonline.com/doi/citedby/10.1080/08941920.2015.1095377?scroll=top&needAccess=true. [Accessed: 24-Sep-2024].
[3] Porter, G. "Health Impacts of Pedestrian Head-Loading: A Review of the Evidence with Particular Reference to Women and Children in Sub-Saharan Africa." [Online]. Available: https://mit.primo.exlibrisgroup.com/discovery/openurl?institution=01MIT_INST&vid=01MIT_INST:MIT&id=pmid:23702214&sid=Entrez:PubMed. [Accessed: 24-Sep-2024].
[4] 2024, "What are spondylolisthesis treatments?," Cleveland Clinic [Online]. Available: https://my.clevelandclinic.org/health/diseases/10302-spondylolisthesis. [Accessed: 24-Sep-2024].
[5] "Degenerative Disc Disease." [Online]. Available: https://my.clevelandclinic.org/health/diseases/16912-degenerative-disk-disease. [Accessed: 24-Sep-2024].
[6] "Lordosis (Swayback)." [Online]. Available: https://my.clevelandclinic.org/health/diseases/23908-lordosis. [Accessed: 24-Sep-2024].
[7] Lai, C., "Water Scarcity in Africa: Causes, Effects, and Solutions." [Online]. Available: https://earth.org/water-scarcity-in-africa/. [Accessed: 24-Sep-2024].
[8] Graham, J., "An Analysis of Water Collection Labor among Women and Children in 24 Sub-Saharan African Countries."

[Online]. Available: https://journals.plos.org/plosone/article?id=info%3Adoi%2F10.1371%2Fjournal.pone.0155981#sec006. [Accessed: 24-Sep-2024].
[9] Russel, K., “Estimating Energy Expenditure of Head-Hauling Water and Grain Grinding from Heart Rate Monitor Measurements in Northern Mozambique.” [Online]. Available: https://pubmed.ncbi.nlm.nih.gov/32611478/. [Accessed: 24-Sep-2024].
[10] Hallett, V., “Millions Of Women Take A Long Walk With A 40-Pound Water Can,” NPR. [Online]. Available: https://www.npr.org/sections/goatsandsoda/2016/07/07/484793736/millions-of-women-take-a-long-walk-with-a-40-pound-water-can. [Accessed: 24-Sep-2024].
[11] “The Gait Cycle.” [Online]. Available: https://www.physio-pedia.com/The_Gait_Cycle. [Accessed: 24-Sep-2024].
[12] Queen, R., “Gender Differences in Plantar Loading During an Unanticipated Side Cut on FieldTurf.” [Online]. Available: https://pubmed.ncbi.nlm.nih.gov/25961157/. [Accessed: 24-Sep-2024].
[13] Siegal, E., “Throwback Thursday: The Physics of an Inclined Treadmill.” [Online]. Available: https://medium.com/starts-with-a-bang/throwback-thursday-the-physics-of-an-inclined-treadmill-2dd2dfe1594d. [Accessed: 24-Sep-2024].
[14] “What Is the Average Walking Speed of an Adult?” [Online]. Available: https://www.healthline.com/health/exercise-fitness/average-walking-speed#average-speed-by-sex. [Accessed: 24-Sep-2024].
[15] “What is a Steep Grade for Hiking: An Empowering and Clear Explanation.” [Online]. Available: https://hikemuse.com/what-is-a-steep-grade-for-hiking/. [Accessed: 24-Sep-2024].
[16] Hirasaki, E., “Effects of walking velocity on vertical head and body movements during locomotion.” [Online]. Available: https://pubmed.ncbi.nlm.nih.gov/10442403/. [Accessed: 07-Dec-2024].